Chapter 11

High-Energy and Short-Pulse Generation from Passively Mode-Locked Ytterbium-Doped Double-Clad Fiber Lasers

Yuzhai Pan

Additional information is available at the end of the chapter

http://dx.doi.org/10.5772/63900

Abstract

Mode-locked ytterbium-doped fiber lasers capable of producing nanosecond-, picosecond- or femtosecond-level pulses with high energy or power have many advantages for various applications such as material processing and laser surgery. Firstly, in this chapter, the principles and methods used in passively mode-locked fiber lasers are briefly described. Secondly, mathematical modeling of all normal dispersion ytterbium-doped fiber lasers for analyzing the pulse generation and propagation has been established and simulated with the generalized nonlinear Schrödinger equation. Thirdly, short pulses generated from passively mode-locked fiber lasers have been demonstrated with carbon nanotube– deposited D-shaped fiber as the saturable absorber. Different pulse width can be realized with different parameters of the laser cavity. Finally, the main amplification methods for short laser pulses have been discussed, and a broad prospect for applications of various technologies using short-pulse fiber lasers is further introduced.

Keywords: Ultra-short pulse, passively mode-locked fiber laser, carbon nanotube saturable absorber, double-clad ytterbium-doped fiber

1. Introduction

Optical fiber lasers gained by rare-earth-ions-doped fibers with broad gain spectrum of tens of nanometers make them very attractive for ultrashort-pulse generation via the mode-locking mechanisms [1, 2]. They are under a growing interest because of their unique features of high efficiency and low consumption, good beam quality, high stability, naturally fiber coupled

and providing a powerful tool for high-speed optical communications, precise micromachining, biomedical imaging, and other applications [3].

Mode locking refers to phase locking of many different frequency modes in a laser cavity, which induces a laser to produce a continuous train of extremely short pulses. Unlike the Q-switched pulses, the mode-locked pulses are phase coherent with each other. Active and passive mode locking are two different methods of mode locking. Active mode-locking methods typically involve using external modulators, for example, electro-optical modulator, which induce a phase or amplitude modulation of the intra-cavity light including lots of longitudinal modes with a periodic duration according to the cavity length to generate the mode-locked pulses, whereas in passive mode locking, the generation of the mode-locked pulse is controlled by the saturable absorber (SA), that is a nonlinear optical element whose loss depends on the laser pulse intensity and causes self-modulation of the light.

Optical pulses generated from passive mode locking have the phase locking being carried out automatically in the cavity without external electrical components required, which results in extremely short and high stability. A number of potential operating and applying characteristics of passively mode-locked fiber lasers have been attractively demonstrated that produce laser pulses with durations from nanosecond to femtosecond, ultrawide bandwidth (~100 nm) at repetition rates ranging from several kHz to hundreds GHz. The research field in passive mode-locking fiber laser goes beyond the generation mechanisms and pulse behaviors that can be found in their operation. A lot of attempts and explores have been made to optimize the operation of the laser to suit for the particular application.

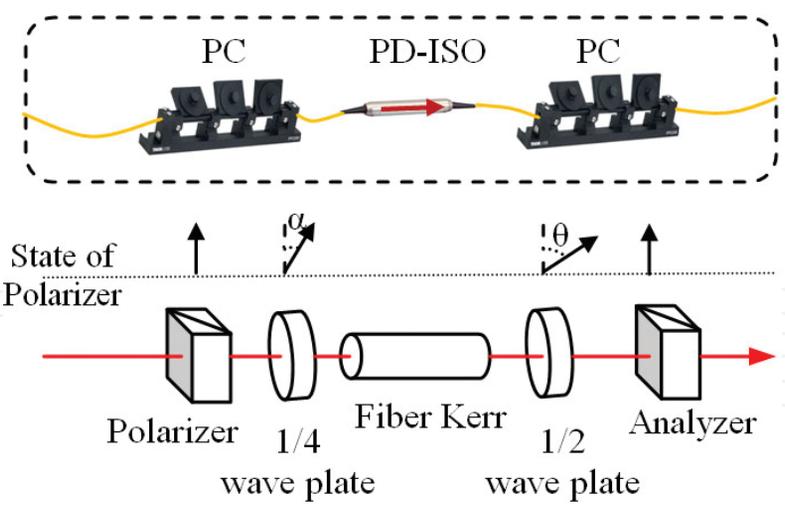

Figure 1. Basic configuration of fiber-based nonlinear polarization rotation. Top, basic configuration; bottom, principle model. PC, polarization controller; PD-ISO, polarization-dependent isolator.

The first passively mode-locked fiber laser was demonstrated in 1983 [4]. An all-fiber, unidirectional, mode-locked ring laser was first constructed using a type of artificial saturable absorber, which uses the effect of intensity-dependent polarization mode coupling in the fiber, that is, nonlinear polarization rotation effect [5]. Since self-phase modulation and other

http://dx.doi.org/10.5772/63900

nonlinearity effects contribute to changing the refractivity index by field intensity, as well the change of the state of polarization as shown in **Figure 1**. Another type of common saturable absorber is based on the nonlinear interference between two polarization modes, that is, the so-called nonlinear optical loop mirror [6] and nonlinear amplifying loop mirror [7]. Nonlinear optical loop mirror relies on the nonlinear interference of the fields that counter-propagate, so the intensity of the pulse is determined by the product of loop length, peak power, and splitting ratio. The longer the loop length, the smaller the peak power required to reach the first transmission maximum. For passively mode-locked fiber lasers operating at large normal dispersion, a short loop length is preferred for ultrashort-pulse generation, while nonlinear amplifying loop mirror is designed with a gain medium placed asymmetrically in the Sagnac loop that is a ring-cavity interferometer. To date, this artificial saturable absorber continues to be an effective approach to generate ultrashort pulses from passively mode-locked fiber lasers [8].

Other methods of the use of new materials have been extensively investigated. Most commonly passive mode-locking devices used in research laboratories and commercial fiber or solid-state lasers are semiconductor saturable absorber mirror (SESAM) [9]. A semiconductor absorber mirror consists of semiconductor heterostructures embedded by a multiple-quantum-well structure like GaInNAs/GaAs. Such a semiconductor absorber mirror can achieve a recovery time of less than 1ns, but has some restrictions on the relatively narrow bandwidth operation, the lower antidamage threshold. Even so, semiconductor absorber mirrors have become widely commercially available and popularly utilization for environmentally robust and stable mode locking.

Various kinds of low-dimensional materials exhibiting the advantages of ultrafast recovery time and broadband saturable absorption have been presented for mode-locked fiber lasers, including carbon-based nanomaterials, such as carbon nanotubes [10], graphenes [11]. Recently, many two-dimensional (2D) layered materials have been investigated as broadband saturable absorbers for the mode locking [12–14]. Almost at the same time, another kind of nanomaterials, that is, the so-called topological insulators (TI), are characterized by a linear dispersion band structure with the Dirac point similar to graphene, which possess inherent features of broad response with a flat broadband wavelength absorption as well as high flexibility. This type of material includes bismuth telluride (Bi_2Se_3) and antimony telluride (Sb_2Te_3) [15, 16]. The manufacturing technique of these low-dimensional materials may have more simple process, easy integration, higher modulation depth, higher damage threshold, a broadband wavelength operation.

Most of passively mode-locked fiber lasers are based on a ring-cavity configuration, which conventionally contains a wavelength division multiplexer for the delivery of the pump energy to the cavity, a segment of gain fiber with the core doped by rare-earth ions, an isolator that provides the unidirectional travelling wave inside the cavity, a beam splitter for the output, a polarization controller, and a saturable absorber for the mode locking. In addition, a spectral filter or other optical elements may be inset into the cavity for the lasing stabilization. In an all-fiber scheme, the cavity contains the active medium and few fiber elements, which offer lower loss for laser pulses. For mode-locked ring-cavity fiber lasers, the fundamental repeti-

tion rate is determined by its cavity length L, the relation expression is as follows: *repetition rate* $=c/nL$, where c and n represents the speed of light, and refractive index respectively. On the state of the so-called harmonic mode locking (HML), the repetition rate can be two or more integer times of the fundamental repetition rate.

To improve the performance of the interaction of nanomaterials and light in fibers, various types of nanomaterial-based saturable absorbers have been demonstrated. For instance, a transmission-mode film-like saturable absorber is fabricated by nanomaterial-polymer composites sandwiched between two fiber ferrules in a standard fiber connector [10, 11]. **Figure 2(a)** shows the typical configuration of a transmission-type saturable absorber. This composite can be constituted by several easy fabrication and integration methods of sputtering, direct synthesis or deposition on the end surfaces of optical fibers, whereas there is a direct physical contact, that is, the laser light is directly transmitted through the nanomaterial film. It is noticed that there may be thermal and mechanical damages within the limited interaction length for high-energy pulsed fiber lasers. A promising alternative is lateral interaction with the evanescent waves of the fiber. The saturable absorbers with the evanescent wave interaction have been demonstrated by several fiber structures including tapered fiber [11], D-shaped fiber [13], etc. The structures and lateral interaction process of the tapered and D-shaped fibers are shown in **Figure 2(b)** and **(c)**. The evanescent wave is generated by total internal reflection of rays at the boundary of the fiber core with a lower index of clad medium. The nanomaterials like carbon nanotubes that contained in the lower-index region can raise the nonlinear reflection coefficient due to evanescent wave absorption along the fiber in a longer nonlinear interaction length in a centimeter scale. This configuration is compatible with the fiber format and easy to add the saturable absorber in the cavity by using simple fiber fusing splicing technique.

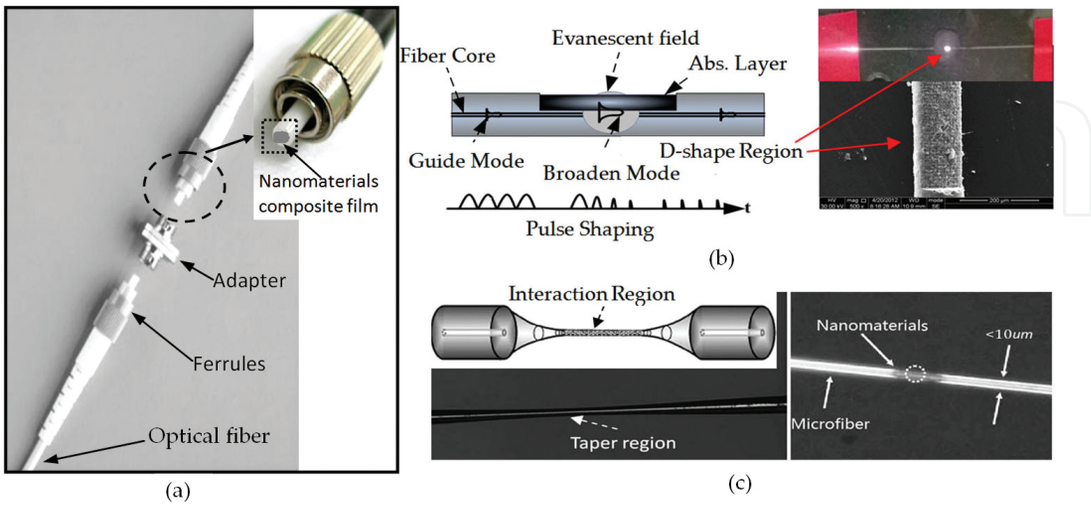

Figure 2. Typical configuration of transmission-type saturable absorber (a), evanescent field interaction of the D-shaped fiber (b), and tapered fiber (c).

http://dx.doi.org/10.5772/63900

Mode-locked silicate-based fibers lasers doped by rare-earth ions have been demonstrated directly operating around 1 μm, 1.5 μm, and 2 μm with very high optical efficiencies. There have also been reported that mode-locked fiber lasers based on Raman cascading, frequency conversion, and other nonlinear processes. The group velocity dispersion of silica fiber is normally positive at 1 μm. Many studies have demonstrated that all-normal dispersion passively mode-locked fiber lasers can generate various kinds of pulses [17], like dissipative solitons, similaritons, noise-like solitons, and soliton rains.

Dissipative soliton pulses refer to those confined wave packets of light in nonlinear optical systems with the balance of nonlinear gain, loss mechanisms. Dissipative solitons generally show large linear chirp with high pulse energies due to the large dispersion experienced in the fiber cavity and possible realization of larger compression ratio by means of simple chirp pulse compression techniques. Dissipative solitons offer highly desirable properties for some direct application and as the seed laser for pulse amplifier system, such as short light pulses of high pulse energies and the improved output stability with compactness, efficiency, and reliability.

An effective method of reducing the repetition rate of passively mode-locked fiber laser is to elongate the cavity by simply adding fiber lengths, and at this time, high-energy ultrashort pulses can be obtained by this effective approach. This method is well suited for fiber lasers where the resonator cavity may reach length in excess of one mile and generate higher energy pulse while maintaining a compact structure [18]. All-normal dispersion passively mode-locked ytterbium-doped fiber laser in a sense offers an ideal laser source of low repetition rate, long duration, and high-energy pulses suitable for a range of applications.

Passively mode-locked fiber laser yields a relatively lower pulse energy in the ultrashort duration because of mode confinement of conventional single-mode fiber. Also, the longer fiber enhances nonlinearities like stimulated Raman scattering and self-phase modulation, which lead to the distortions of the pulse and instability of the mode locking. Today, for the sake of the high-energy laser pulses with available pump power in many application fields like micromachining, many researchers pay their attentions to the use of double-clad fiber for high-power fiber amplifiers and lasers. The double-clad fiber can be pumped by high power laser diodes to get the higher gain [19–21], where the pump light is coupled into the larger inner cladding with a higher numerical aperture.

2. Simulation of passively mode-locked ytterbium-doped fiber laser

Ultrashort-pulse propagation in optical fiber can be accurately modeled by one or more coupled partial differential equations. Various of simulation methods with different theoretical models have been introduced to study laser pulse phenomenon and dynamic processes in the cavity with the parameters of dispersion, nonlinearity, gain, loss, etc. The well-known master mode-locking equation first proposed by H. A. Haus [22], which being a perturbation from the nonlinear Schrödinger equation, has the capacity of describing both the energy saturation and the pulse stabilization process. To prove the possibility of stable pulse gener-

ation in the presented cavity, numerical simulation of the generalized nonlinear Schrödinger equation is performed here, which provides an insights into the mode-locking dynamics of ytterbium-doped fiber lasers and directs to the performance optimization for the pulses.

The whole cavity is schematically shown as an analytical model in **Figure 3**. The main parameters of each fiber can be found in **Table 1**. Firstly, we have numerically simulated the pulse propagation and formation in the cavity governed by the following equation [23]:

$$\frac{\partial A}{\partial z} = \frac{g-\alpha}{2} A + \frac{g}{2\Omega_g^2}\frac{\partial^2 A}{\partial \tau^2} + i\gamma |A|^2 A - i\frac{\beta_2}{2}\frac{\partial^2 A}{\partial \tau^2} + i\frac{\beta_2}{2}\frac{\partial^3 A}{\partial \tau^3} \quad (1)$$

where A is the slowly varying envelope of the optical field, z is the axial distance, τ is the local time, α accounts for the loss, γ is the nonlinear coefficient of fiber, which accounts for the self-phase modulation effect, and β_2 is the second-order derivative of the propagation constant. During each cavity round-trip time, the pulse goes through different cavity components, and the output from one component is used as the input to the other, as described in **Figure 3**. Also, the pulse goes through the saturable absorber with a nonlinear loss and through the coupler with a fraction of the pulse energy outputted. The fiber parameters were chosen to match the measured or specified parameters of different elements used in the experiment.

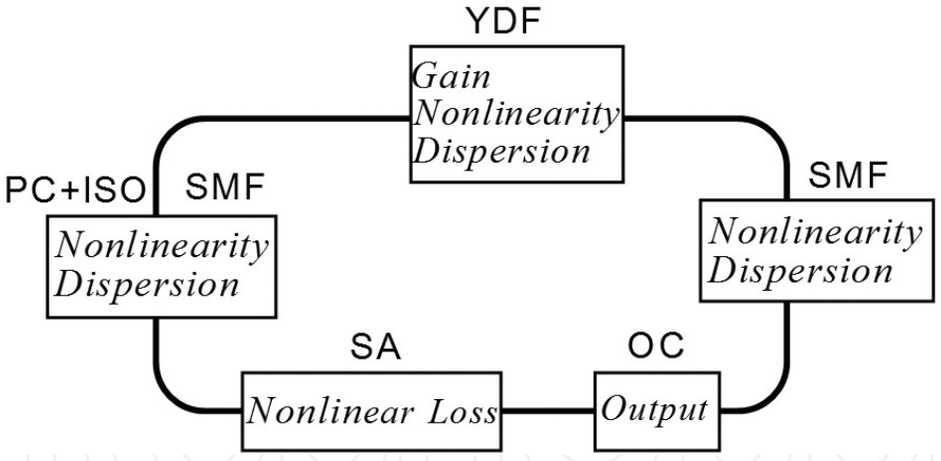

Figure 3. Proposed model of passively mode-locked fiber laser. YDF, ytterbium-doped fiber; SMF, single mode fiber; OC, output coupler; SA, saturable absorber.

Fiber type	β_2 (ps^2 m^{-1})	β_3 (fs^3 m^{-1})	γ (W^{-1} m^{-1})	Length (m)
Ytterbium-doped fiber	0.021	0.0254	0.0048	10
Other fiber elements	0.022	0.0254	0.0044	5
Hi1060 fiber	0.022	0.0254	0.0044	20 or Var.

Table 1. Summary of the fiber parameters used in the simulation.

http://dx.doi.org/10.5772/63900

The parameter g denotes the gain coefficient of ytterbium-doped fiber, which can be described as the gain function and approximately expressed by:

$$g_i = \frac{g_0}{1 + E_{pulse} / E_{sat}} \tag{2}$$

where E_{sat} is the saturation energy due to the limited pump power, which is defined as $E_{sat}=(h\nu/\sigma)A_{eff}$ with the dependence of pump power. The pulse energy E_{pulse} is given by $E_{pulse}=\int_{T_R/2}^{-T_R/2} |A(z,\tau)|^2 d\tau$, where T_R is the cavity round-trip time. The same small signal gain g_0, depending on the doping concentration, can be assumed to be constant if only a small fraction of the pump light is absorbed provided an approximation of uniform pumping. Ytterbium-doped fiber is modeled with a total unsaturated gain of 30 dB, corresponding to these parameters: $g_0=6.9m^{-1}$ and $E_{sat}=1nJ$. Ω_g is the gain bandwidth of ytterbium-doped fiber, which is related to the bandwidth $\Delta\lambda$ through $\Omega_g=|2\pi c/\lambda^2|\Delta\lambda$, where $\Delta\lambda$ is chosen to be 55nm bandwidth.

The parameter β_2 represents dispersion of the group velocity contributing to time-domain broadening of laser pulse, that is, the so-called group velocity dispersion, which is commonly used by physicists in units of $ps^2\Delta m^{-1}$. For optical fibers, the group velocity dispersion usually refers to the chromatic dispersion parameter D that defined as a derivative $d\beta_1/d\lambda$, which is also used in practice with the relation of β_2 and n as: $\beta_2=-(\lambda^2/2\pi c)\Delta D$, where λ is the operating wavelength. The higher order dispersion and higher order nonlinear effects were ignored in simulations. Fiber nonlinear parameter γ relates the wavelength λ and effective area A_{eff} to the nonlinear index n_2 with an expression as: $\gamma=2\pi n_2/\lambda_0 A_{eff}$, when the radial field distribution is known.

Nonlinear transmission of the saturable absorber can be described by $T=\exp[-(\alpha_1+\alpha_{nl})]$, where α_1 is nonsaturable absorption loss, and α_{nl} denotes power-dependent nonlinear absorption loss, which is given by $\alpha_{nl}=\alpha_0/(1+P(\tau)/P_{sat})$, where α_0 is the saturable loss due to the absorption, that is, the modulation depth. $P(\tau)$ is the instantaneous pulse power and P_{sat} is the saturation power of the saturable absorber. The saturable loss, which acts as an equivalent-filtering effect, has a significant impact on the pulse duration and bandwidth of laser pulse. It is expected, for high power/energy pulse, that the saturable absorber with a larger modulation depth can be used in a fiber laser with large normal dispersion and strong nonlinearity. The further increase of the modulation depth should be carefully designed due to the limitation of the nonsaturable loss. One probable way for the increase of modulation depth is to reduce the evanescent field leaking of D-shaped fiber and enlarge the evanescent field interaction with the saturable absorber by lengthening the fiber D-shaped domain. Here, the parameters of the saturable absorber in the simulation model are as follows: $\alpha_1=45\%$, $\alpha_0=27\%$, and $P_{sat}=1000W$.

2.1. Numerical simulation and results

All optical fibers in the model above have normal dispersion within the laser spectral range. A 20 m length of Hi1060 fiber was inserted into the cavity aiming to increase the cavity length. The total dispersion is calculated to be about 0.75 ps^2. Eq. (1) has been solved with the standard split-step Fourier method. The simulation field is represented on a temporal grid (and via the Fourier transform on a frequency grid) consisting of 2^{11} points with a width of 0.2 ns. One initialized weak signal was introduced into the round-trip propagation in the cavity, and this pulse consecutively experiences each action of cavity components along the routes.

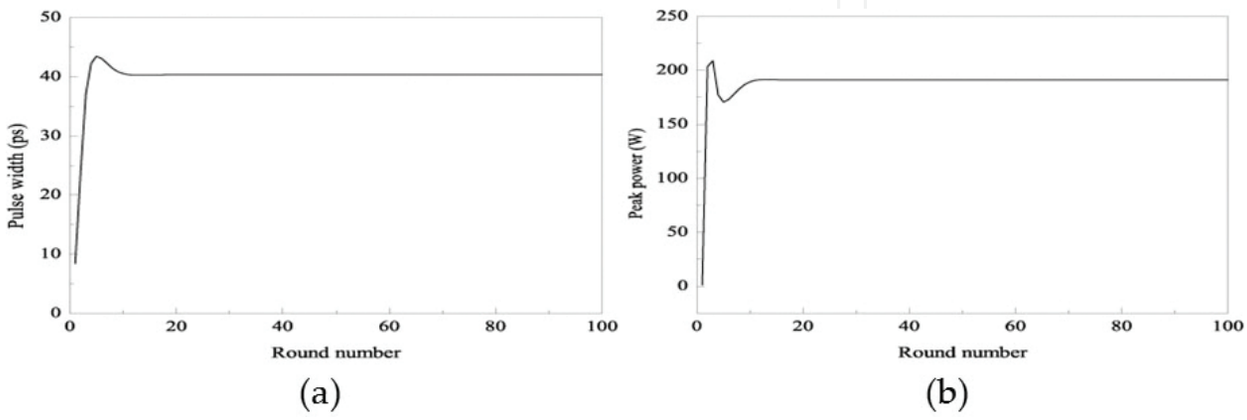

Figure 4. Transient evolution of the pulse width (a) and peak power (b).

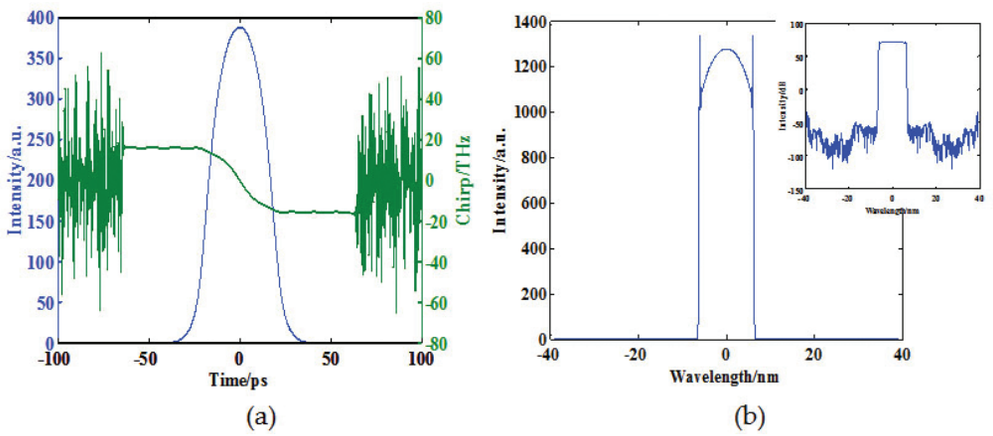

Figure 5. Pulse profile and chirp (a), and spectrum (b) of mode-locked laser. The inset is the spectrum in decibel scale.

After a finite number of round trips, the pulse started to converge into stable dissipative soliton solutions. The simulation results indicate that stable solutions do exist in such a laser, which can be confirmed from the peak power and pulse duration evolutions as shown in **Figure 4**. The pulse duration is ~40.6 ps and the spectral edge-to-edge bandwidth is 11.2 nm as shown in **Figure 5**, which both evidently indicate that the pulses are highly chirped. As shown in **Figure 5(b)**, the spectrum on a linear scale and a logarithmic scale is characterized by their

http://dx.doi.org/10.5772/63900

steep edges, that is, the so-called M-shaped optical spectra. The higher peak power of the pulse after amplification by gain fiber induces a substantial nonlinear phase shift in the single-mode fiber, which results in sharp peaks on the spectrum edges. The gain and loss coexist in the dissipative system and play an essential role in the formation of dissipative solitons. Thus, dissipative soliton must be self-organized and its dynamics differ from that of the conventional soliton. It is noted that the saturable absorber has a nonlinear transmission depending on the light intensity, and the nonlinear phase shift is gradually varied in the process of gain saturation when an initial pulse is circulating in the cavity [24].

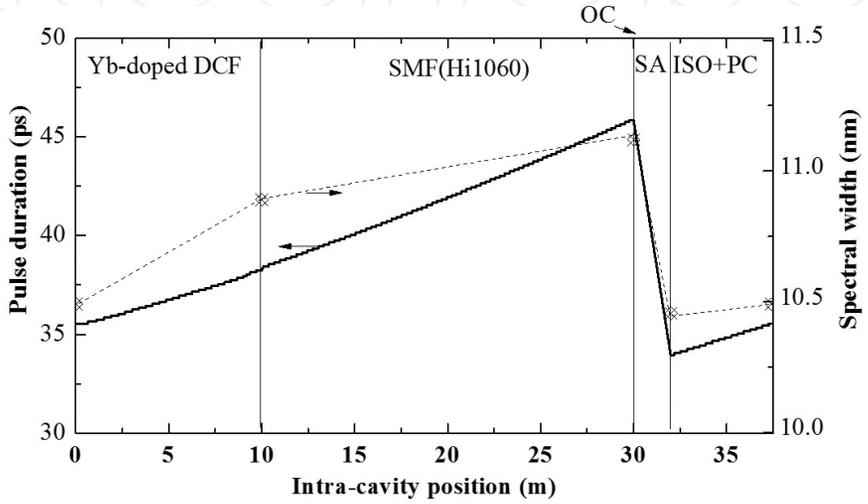

Figure 6. Evolution of the pulse width and spectral bandwidth in one cavity round trip.

The evolutions of the pulse duration and spectral edge-to-edge bandwidth in one cavity round trip are shown in **Figure 6**. It can be seen that the significant broadening of the duration and spectral width of the pulse after passing through the gain fiber. The large normal dispersion of a long segment of single-mode fiber induces large and positive chirp. The nonlinear phase shift broadens the spectrum of the pulse, while strong chirping induced by normal cavity dispersion enlarges the pulse pedestals, which are the lower intensity red-shifted and blue-shifted spectral weights located at both pulse edges in time-domain. When the pulse is travelling throughout the saturable absorber, pulse duration and spectrum width could be compressed. Here, the saturable absorber plays a key role of providing an effective filtering function to stabilize the mode locking.

When the cavity length was increased to 60m, the total cavity dispersion is up to ~1.3 ps^2. The laser works on a larger normal dispersion regime without dispersion compensation in this model as the same above. Simulation results showed that the stable pulse obtained with the pulse duration of 76.5 ps and the corresponding spectral width of 9.6 nm. With the larger positive dispersion, the stable pulses have been obtained again but highly chirp. Comparing the pulse characteristics of these two cavities, the broadened pulse induced mainly by self-phase modulation in the longer cavity has lower peak power, and both of the equivalent filter effect and lower self-phase modulation result in the narrower spectrum.

For the deliverable high energy of the pulse, the stabilization of mode locking should be ensured in a normal and large cavity dispersion accompanied with a high nonlinearity. A spectral filter, which is added in such a laser cavity, can be considered as an effective absorber in the spectral domain to cut off the temporal wings of the pulse and stable the mode locking. It is assumed that the spectral filter has a Gaussian profile, so the spectral filter is numerically implemented in the model by a function as: $T(\omega)=\exp[-(\omega/\Omega_f)^2]$, where ω is the angular frequency, and Ω_f is the bandwidth of the spectral filter. The influence of the spectra filtering on pulse shaping could be investigated for the stabilization of the mode locking, as well as the performance optimization of the pulses [25].

3. Mode-locked ytterbium-doped fiber laser with carbon nanotubes

Single-walled carbon nanotube is an enrolled two-dimensional graphene honeycomb sheet with a diameter of typically 0.6–2 nm and a length distribution ranging from tens of nanometers to several micrometers. Depending on their chirality [26], single-walled nanotubes exhibit two different electrical properties, metallic or semiconducting. Semiconducting nanotubes have an energy band gaps like those in ordinary semiconductors; thus, photons having corresponding wavelength are absorbed. Single-walled nanotubes are a kind of promising material as saturable absorber for passive mode locking because the bandgap energy can be controlled by the tube diameter, which would be applied for different spectral ranges.

The absorption loss and modulation depth of the nanotubes-based saturable absorber can be adjusted by changing the concentration of nanotubes, the interaction length of light with nanotubes, nonsaturable loss of fiber structure, and substrate materials. To study the effect of modulation depth on the mode locking in a larger normal dispersion cavity with high nonlinearity, the evanescent field used here is from the D-shaped fiber that was fabricated by ablating part of the cladding of single mode fiber by the femtosecond laser-induced water breakdown method [27]. Top- and side-view microscope images of the as-prepared D-shaped fiber are shown in **Figure 7(a)**. Averaged distance between the core and the flat face of the fiber is about 7 μm, and the entire length of D-shaped fiber is 900 μm. Measured insertion loss of the D-shaped fiber is about 0.6 dB which guarantees the lower loss in the cavity. Secondly, the commercial solution of single-walled carbon nanotubes with the purity of approximately 95% was used in the experiments. The diameter distribution of nanotubes is around 1.5 nm. The nanotube solution was further diluted to be a concentration of 0.05 wt% with a ten-hour ultrasonically agitated process to minimize bundling of nanotubes. Finally, the well-dispersed aqueous solution was sprayed on the D-shaped surface of the fiber. These devices were dried out in a vacuum oven at the temperature of 40 °C for 30 min carefully adjusted to reduce agglomeration and detaching of nanotubes. Simple encapsulation for these saturable absorbers was performed to avoid unexpected damage. A microscope image of the nanotube–deposited D-shaped fiber is shown in **Figure 7(b)**. The transmission values of the saturable absorber were recorded by using the ultrashort-pulse fiber laser with a MHz repetition rate at different average power. The results for both the D-shaped fiber with nanotubes and with-

out nanotubes are presented in **Figure 7(c)**. The result shows that the transmissivity can be changed with the increase of the input power indicating the existence of saturable absorption. The power-dependent transmissivity induced by nanotubes can be decreased to ~28%. Nonsaturable loss induced by both D-shaped fiber and other impurities is about 21%. The modulation depth of about 51% can be provided, which is higher and sufficient.

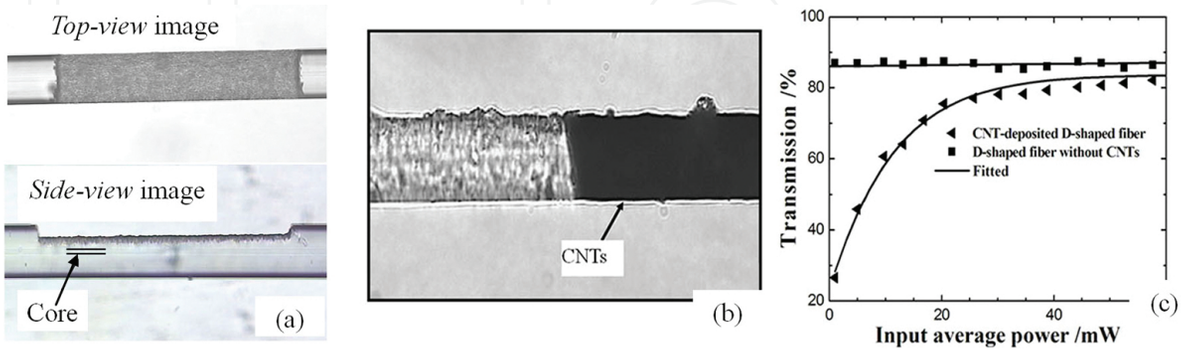

Figure 7. (a) Top-view and side-view microscope images of a D-shaped zone in fiber, (b) microscope image of carbon nanotube–deposited D-shaped fiber, and (c) transmissivity curves of saturable absorber and D-shaped fiber versus the input power.

3.1. Ultrashort-pulse generation

The presented experimental setup is schematically shown in **Figure 8(a)**. A side-pumping scheme of ytterbium-doped fiber was taken as the gain fiber pumped by 915-nm laser diode through a fiber combined with a coupling efficiency of 90%.

A lower absorption coefficient of gain fiber could suppress thermal effects to some extent, a 10-m-long ytterbium-doped double-clad fiber (Nufern SM-YDF-5/130) with a cladding absorption coefficient of 1.16 m^{-1} at 915 nm. The dispersion and nonlinear coefficients of ytterbium-doped fiber are $0.02 ps^2 \cdot m^{-1}$ and $0.0048 W^{-1} \cdot m^{-1}$, respectively. A 20-m-long single-mode fiber was employed to extend the cavity length, which correspondingly decreased the repetition rate. An optical coupler (OC) provided a 20% output ratio. The dispersion and nonlinear coefficients of single-mode fiber are $0.022\ ps^2 \cdot\ m^{-1}$ and $0.0047\ W^{-1} \cdot m^{-1}$, respectively. The total length of laser cavity is ~36.5 m with the all-normal cavity dispersion of ~0.76 ps^2.

Self-starting mode locking has been achieved at the pump power of ~0.6 W by appropriately adjusting polarization controller. The self-consistent pulse evolution and stable mode locking indicate that the saturable absorber performs a filtering-equivalent function by the loss depending on light intensity to promote and stabilize the mode-locking operation in all-normal dispersion cavity as we expected. The pulse train generated has been observed by the oscilloscope trace as shown in **Figure 8(b)**. The pulse sequence was traced up to 2.5 μs by an oscilloscope connected with a high-speed photodetector (3 GHz). The figure exhibits the round-trip time of ~178.7 ns corresponding to the repetition rate of 5.59 MHz, which is consistent with the cavity length.

The temporal profile and spectral of the pulse recorded at the pump power of 2 W are shown in **Figure 8(c)** and **(d)**. The spectrum was measured by a spectrometer with the resolution of 1 nm (Ocean Optics Inc., HR4000). The operation wavelength is around 1085 nm, which indicated nearly four energy-level lasing behavior of ytterbium ions. The pulse duration is 46.6 ps, and the spectrum has an approximately M-shaped profile on a linear scale with a bandwidth of ~12.8 nm, which implies that the mode-locking operation in the dissipative soliton regime. The pulse duration could be further decreased to 941 fs from the outside cavity simple compression by using a segment of single-mode fiber with negative dispersion. The near Gaussian fitting shape of the pulse suggests that linear chirp dominates across the pulse in the cavity.

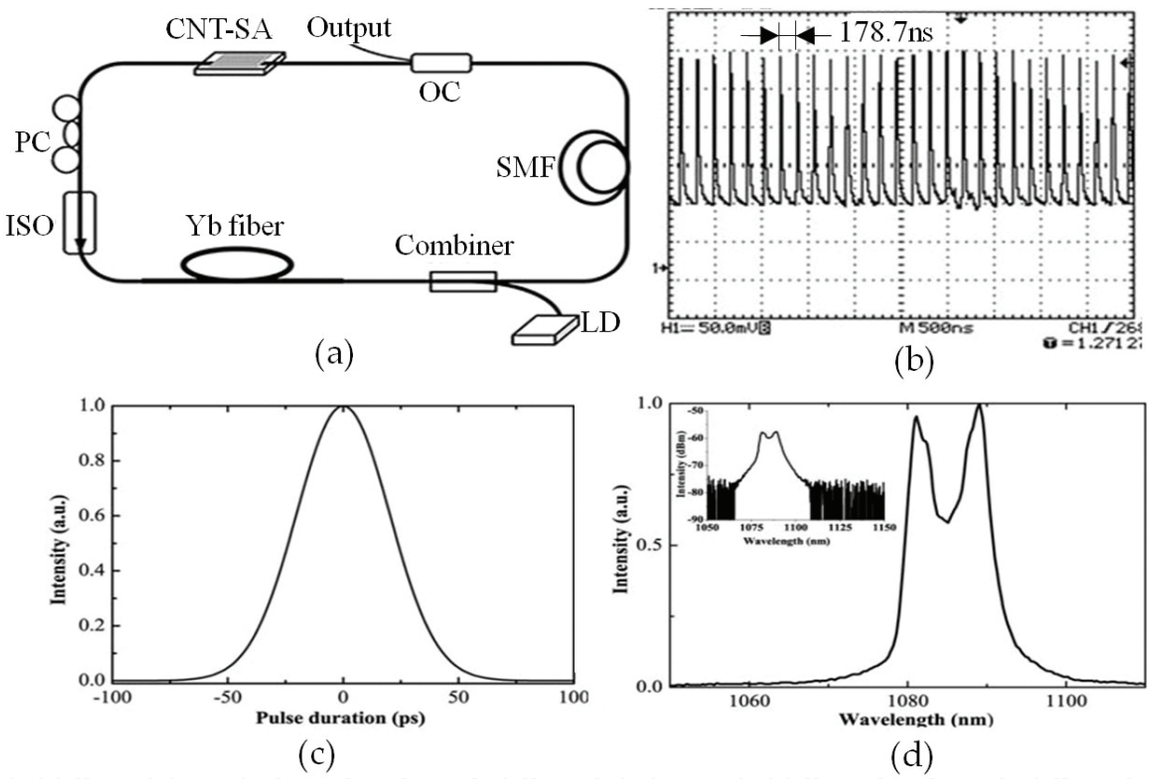

Figure 8. (a) Schematic diagram of mode-locked fiber laser, (b) oscilloscope traces of pulse train, (c) pulse profile trace of the pulse, and (d) output spectrum (the inset is the spectrum in a log scale).

When the pump power was increased to 3.5 W, the corresponding pulse duration was enlarged to 62.6 ps, and the spectral width was broadened to 16.3 nm. The output power was almost linearly increased to 162 mW, and the corresponding pulse energy was raised to ~29 nJ. The experimental results manifest that the evanescent-field interaction scheme and large modulation depth of the saturable absorber would be preferentially chosen for the achievement of high-energy pulses. Mode-locked fiber lasers could be robust against optical wave breaking due to the linear chirp across the pulse, showing a stretched pulse with the duration up to a few or even several hundred picoseconds.

http://dx.doi.org/10.5772/63900

Unlike nonlinear polarization rotation effect, various new nanomaterials hardly generate fs-level ultrashort pulses directly from the laser oscillators [28]. A robust self-starting picoseconds ytterbium-doped fiber laser is easy to be realized by using one of other 2D materials or topological insulators, at the aspect of characteristics of the pulses, those results are similar to these of carbon nanotubes yet. The pulse duration is limited by large normal dispersion, while the larger linear chirp dissipative solitons pulses are easy to be compressed. So the research interests are focused on various pulses dynamics of stable, self-starting mode locking of the fiber lasers in all-normal dispersion regime.

3.2. Nanosecond-level pulse generation

Carbon nanotubes have been demonstrated it suitable for stable long-duration pulse mode locked in all-normal dispersion regime [29]. Absence of nonlinear polarization evolution dynamics gives giant chirped pulses that can be suitable for compression. Here, an ultralong cavity ytterbium-doped fiber laser mode locked by nanotubes-based saturable absorber has been experimentally investigated. It is used a saturable absorber with the unsaturated loss of ~57.8% and the modulation depth of ~4.7%. The ring cavity was elongated by an one-kilometer-long single-mode fiber (YOFC, C1060), which results in an ultralong laser cavity with the length of 1021 m.

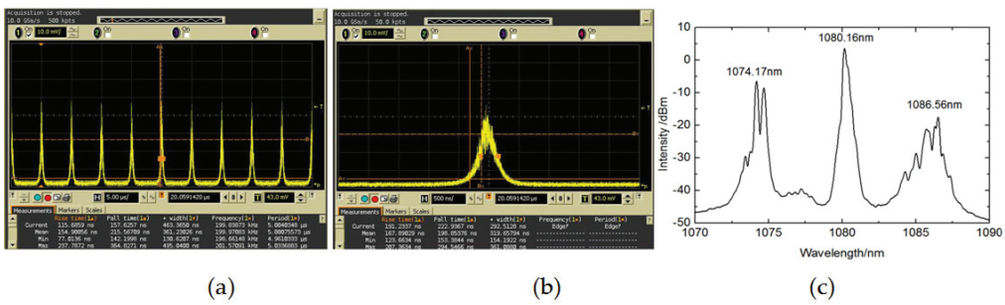

Figure 9. Characteristics of noise-like pulses. Train trace (a), single pulse (b) and optical spectrum (c).

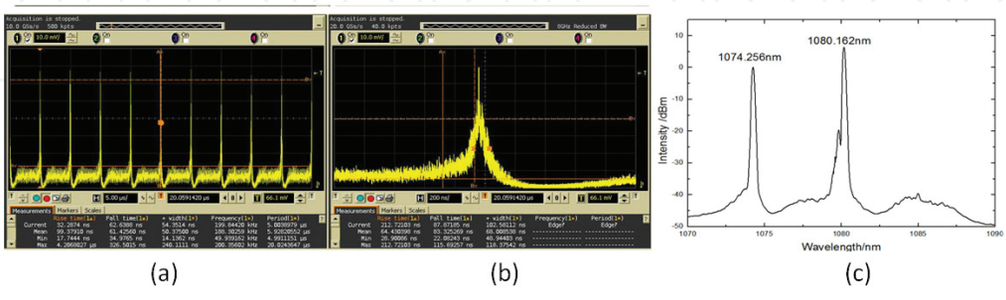

Figure 10. Characteristics of soliton rains. Train trace (a), single pulse (b), and optical spectrum (c).

Stable mode-locked pulses were obtained by slightly adjusting PC at the pump power of 0.81 W. The amplitude of the pulse was increased with the increase of pump power until the

power of 1.81 W, which changing into a state of multipulses. The pulse sequence and single pulse, which is a typical noise-like pulse, have been measured and shown in **Figure 9(a)** and **(b)**, respectively. The repetition period of the pulse is approximately 5 μs. The pulse duration is approximately 292.6 ns. When the pump power was 1.81 W, another stable state, that is, soliton rains, could be obtained with carefully adjusting the polarization controller. **Figure 10** shows the pulse train, single pulse, and the spectrum of the fiber laser at the pumping power of 1.93 W. Within each pulse period, the pulse contains background noise, drifted pulse, and phase-condensed soliton. The intensity of the drifted pulse is about 10% of the phase-condensed soliton. The pulse width of phase condensation soliton is about 102.5 ns at 3 dB, as shown in **Figure 10(b)**. The steady soliton rains cannot be maintained once the pump power is above 1.93 W. The maximum output power is ~40.3 mW with single pulse energy of ~201.5 nJ. Output spectra of the noise-like pulses and soliton rains have been measured and shown in **Figures 9(c)** and **10(c)**. It can be seen that both spectra have several central wavelengths indicating that the presence of filtering effect in the cavity could be used as a multiwavelength short-pulse fiber laser.

Recently, it has been reported that the generated pulses of an ultralong cavity fiber laser can deliver microjoule-level energy in the nanosecond range [30]. In the all-normal dispersion fiber laser systems, the stable mode-locking pulses exhibits that the formation of pulse shaping is the product of complicated processes of energy conversion. Various nonlinear effects such as self-phase modulation, dispersion wave, peak clamping, which have strong influence on the stability of mode locking, and combining with high cavity dispersion can lead to complex pulsing phenomena, like wave-breaking of the soliton pulse as noise-like pulses in the results above. On the other hand, the Raman-induced noise-like pulses can be realized by the Raman effect in a fiber laser with high nonlinearity and dispersion [31].

4. Amplification of short-pulse fiber lasers

Because laser pulses that extracted from the master oscillator are generally of relatively low energies, an additional external amplifier is required for the enhancement of the pulse energy, which is of key importance of power scaling of fiber lasers for the wide applications. Ytterbium-doped fiber laser systems are excellently suited to generate and amplify ultrashort laser pulses due to their large amplification bandwidth supporting pulse durations of few hundred femtoseconds. This approach is benefited from the simple fiber connection between the oscillator and the amplifier. There are mainly two methods, that is, the chirped pulse amplification (CPA) and the master oscillator power amplification (MOPA).

For the CPA technique, ultrashort pulses are amplified by time stretching of the original pulses and later recompress them back into a short duration after the fiber amplifier [32]. The chirped pulse amplifier system, as schematically shown in **Figure 11**, is composed of a seed laser, a pulse stretcher, amplifier chains, and a pulse compressor. The duration of laser pulses is firstly increased temporally to a much longer duration of the order of 1ns, that is chirped by using a pulse stretcher, for example a grating pair, fiber chirped Bragg grating, etc., which reduces the

http://dx.doi.org/10.5772/63900

peak power to a level so that the nonlinear effects in the gain medium can be avoided. The stretched pulse was amplified in next amplifier system, which typically consisted of large-mode area single-mode fiber or photonic crystal fiber (PCF) gained by multimode laser diodes, allowing more peak power generation below the limit of nonlinear optical intensity effects. Finally, a low-loss compressor is used to temporally compress the pulses to a duration similar to the input pulse duration. The pulse stretcher is necessary for the amplification of ultrashort pulses. Or otherwise, high nonlinearities in the fiber induced by high optical peak power in ultrashort pulses would affect the recompression to an ideal short pulse in the final compression part. Of course, the compressor also needs to tolerate high peak powers without introducing nonlinear distortions.

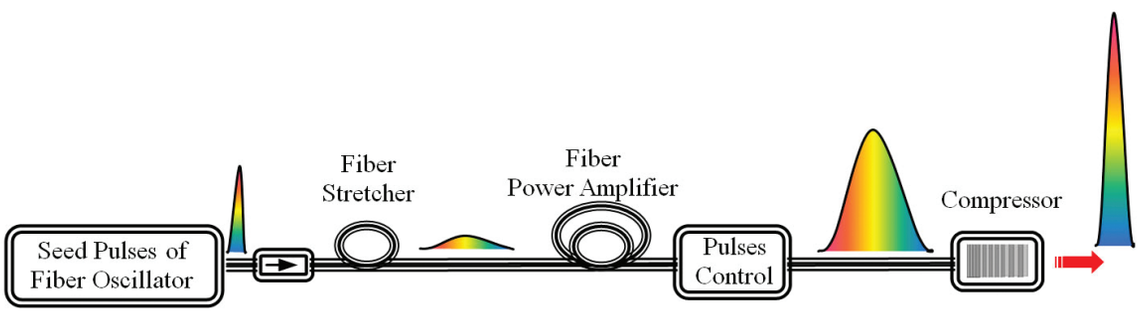

Figure 11. Schematic diagram of the chirped pulse amplifier for ultrashort-pulse fiber laser.

Femtosecond fiber amplifier systems have the potential for millijoule pulse energies at megahertz repetition rate. Fox example, a ytterbium-doped fiber amplifier system has delivered millijoule level pulse energy at repetition rates above 100 kHz corresponding to an average power of more than 100 W, the compressed pulse is as short as 800 fs [33], where a short-length PCF with 80-μm core diameter is employed, which allows the pulse energies up to 1.45 mJ with a stretched pulse duration of 2 ns. Scaling up of pulse energy in an ultrafast fiber laser has been demonstrated that the simultaneous generation of 60 W of compressed average power at 100 kHz, together with 320 fs and 600 μJ pulses [34].

Highly chirped pulse fiber oscillators may create powerful all-fiber generator-amplifier systems, that is, the so-called master oscillator power amplifier (MOPA), which is an attractive technology to achieve picoseconds-level laser pulses with higher average output power and peak power [35–38]. The master oscillator power amplifier, as shown in **Figure 12**, generally consists of a laser oscillator that produces the weak seed pulse and series of amplifiers that increase the laser power to the required level. Chirped pulses from the generator are directly fed to an amplifier without the use of a stretcher or a modulator and compressed after one or more amplifying stages. In addition, the chirped pulses coming out of the master oscillator in the normal dispersion regime, like dissipative solitons, whose energy exceeds the energy of classical solitons by tens or hundreds of times because of longer duration at the same peak power, can be further increased to the required level in one power amplifier, as well compressed by an external compressor.

Double-clad fibers have been extensively used to build fiber amplification systems, exhibiting desirable characteristics such as high gain, good efficiency, and excellent beam quality. A diode-pumped mode-locked ytterbium-doped fiber seed laser followed by two fiber amplifiers has been demonstrated [36], where both fiber amplifiers with the design of large-mode area were cladding pumped. The oscillator produced 30 pJ, 1.8 ps pulses. After two-scales amplifying, the output pulses compressed by 830 grooves/mm gratings produced high-quality 400 nJ pulses with a pulse duration of 110 fs at average power levels in excess of 25 W. A carbon-nanotube-based master oscillator power amplifier has also been reported that a compact picosecond-level pulse fiber laser with high average power [37]. The seed laser that is the nanotube-based mode-locked Nd:YVO_4 laser is further amplified with a single-stage fiber amplifier. An amplified pulse with a pulse width of 15.7 ps, pulse energy of 244 nJ, has been achieved with an average power of 20 W at a repetition rate of 82 MHz. A fiber amplifier contains a seed source and two-scale amplifiers in that the gain fibers are different size double-clad fibers to suppress the nonlinear effects, and single pulse energy of 4.56 μJ with a pulse width of 0.62 ns at 26.3 MHz has been realized [38]. These systems present simple and practical fiber-based solutions for high-average-power ultrashort-pulse laser applications.

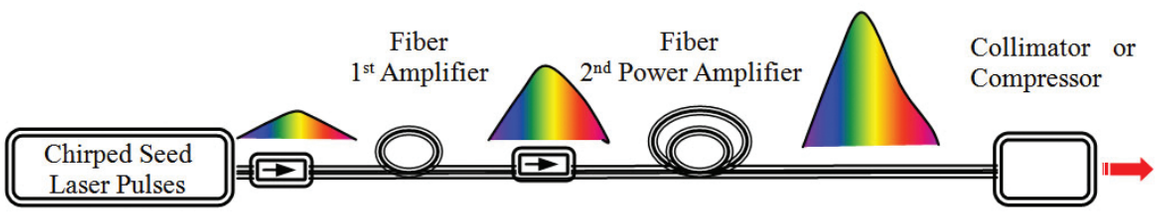

Figure 12. Schematic diagram of a master oscillator power amplifier system.

Fiber nonlinearity is proportional to the length of fiber and inversely proportional to the fiber core size. The developed large-mode area double-clad photonic crystal fiber can be considered as a possible approach to overcome many of the difficulties as mentioned above. These amplifiers enabled by advancements in photonic crystal fiber manufacturing technology can generate kilowatts to multigigawatts of peak power using direct amplification showing excellent conversion efficiency, diffraction-limited beam quality.

5. Typical applications of short-pulse mode-locked fiber lasers

Fiber laser sources with nanosecond pulses have great potential in a variety of applications requiring low temporal coherence, such as optical metrology, or sensor interrogation based on low-coherence spectral interferometry technology. Furthermore, the applications of fiber-based master oscillator power amplifier sources can also extend to industrial fields, such as laser marking, engraving, and other micromachining in various materials, particularly suitable for cutting high reflectivity materials like titanium, copper [39], silver [40]. Other successfully commercial examples include the high-resolution 3D imaging lidar system [41], nonlinear

frequency conversion [42], etc. The pulse duration of ultralong cavity mode-locked fiber laser may be up to several or even hundreds of nanoseconds with higher energy. In contrast to the Q-switched lasers, obviously, there would be the limited range of direct applications. For this reason, the interests would focus on the high-chirp solitons or dissipative solitons resonance with the duration as long as nanoseconds that can further be compressed into a picosecond level.

All-fiber subnanosecond lasers have great potential application in the generation of wide-band supercontinuum (SC) source [38]. The supercontinuum laser source is the widely broadened spectrum generated by strong nonlinear effects using highly nonlinear fibers. The output power of this novel supercontinuum light source is high by using the small core fibers, so that the supercontinuum source is of interest to many kinds of applications. For example, an ultrahigh-resolution optical coherence tomography (OCT) has been investigated by using the ultrashort-pulse fiber supercontinuum source as fiber-based, high-power, wideband sources [43].

Laser beam at the output of the fiber can be easily focused in a spot with a radius of ~μm, a few nanojoules of energy in a tens femtoseconds pulse resulting in intensities on the order of ~GW/cm^2. So, ultrashort laser pulses would not induce heat diffusion during the fast interaction with objects such as various materials and living structures, that is, free from cracks and melting and other thermal effects [44]. For ultrashort laser pulses with the duration below several picoseconds, the pulses interacting period is generally shorter than the lattice heating time, which is necessary for energy diffusion processes for most materials. Ultrashort-pulse fiber lasers presently have provided a stable and reliable platform for many applications.

Material micro- and nano-machining has been for a long time identified as an important and the largest market for high-power/energy ultrashort-pulse fiber lasers [45]. High pulse intensities are widely used for permanent transparent material modification. In addition, these extremely high power densities of the pulses resulting in a highly localized disruption of the material matrix with very little energy deposited and few heat transferred to the surrounding material. This is a so-called laser cold process. A clear processing edge formed by laser ablation is of key importance for medical, photovoltaic, and semiconductor industry, especially for thermally sensitive material, like nitinol shape memory alloys, bio-absorbable polymers like polylactic acids, glass, etc. [46]. In comparison, nanosecond laser pulses micromachining in glass or other materials would leave an undesirable heat-affected zone, numerous stress fractures, and micro-cracks around the processing edge.

Although known as a cold ablation process, by precisely controlling localized heat accumulation to melt material accompanying with the inhibition of shrinkage stress by producing embedded molten pool by nonlinear absorption process, ultrashort laser pulses at high repetition rates (hundreds of kHz and above) have been applied into micro-welding of materials including glass and plastic, silicon and glass, and medical piece part [47].

Ultrashort-pulse laser make them ideal sources for time resolved measurement of the faster physical and chemical phenomenon. By controlling the optical carrier frequency and the carrier phase of ultrafast lasers, optical frequency combs, spectroscopy and precision metrology of

optical frequency transitions and natural constants have been realized. Pump-probe measurements can use ultrashort laser pulses to measure and determine the evolution of a series of ultrafast processes in many kinds of materials, molecules or even in internal states of atoms, with the advantage of shortening the transient behavior resulting from the optical excitation [48]. Femtosecond laser pulses with modest energies generating the intensities above 10^{15} W/cm^2 are used to determine the elements of the sample in a technique called femtosecond laser-induced breakdown spectroscopy (fs-LIBS) [49].

Ultrashort fiber lasers are developing rapidly in the medical and biology applications. These laser pulses can be used as a laser scalpel directly to medical treatment on the one hand. The advantages of accuracy, absence of thermal interaction, and safety have been accepted by a wide customer. On the other hand, the indirect applications refer to high precision and high-quality medical devices, such as stents, implants, and catheters, requiring sophisticated manufacturing techniques, which are available from medical industrial manufacturing processes. An example has been reported in 2014, the multifunctional biochips for realizing high-performance biochemical analysis and cell engineering [50].

In conclusion, passively mode-locked ytterbium-doped fiber lasers operating in the normal dispersion regime have been firmly established in the field of various short-duration pulses, and attracted increasing attention due to their compactness, low cost, and widespread applications. Various technologies have been developed with the aim to realize short-pulse all-fiber laser sources with the desirable energies, durations, average powers and beam quality, as well the environmental stabilization and reliability. This chapter is intended to smoothly understand each topic on this field and has the interest to further read and explore high-energy short-pulse generation and their applications.

Acknowledgements

This work was partially supported by Shandong Graduate Teaching Innovation Project (SDYY15003) and HIT Graduate Teaching Reform Project(JGYJ201436 & WH2015008).

Author details

Yuzhai Pan*

Address all correspondence to: panyzh2002@163.com

Department of Optoelectronic Science, Harbin Institute of Technology at Weihai, Hi-Tech District, Weihai, China

References

[1] S M Swift. Q-switched and mode locked short pulses from a diode pumped, Yb-doped fiber Laser. BiblioScholar; 2012

[2] M J F Digonnet. Rare-earth-doped fiber lasers and amplifiers. 2nd edn. Boca Raton, FL: CRC Press; 2001

[3] H Endert, A Galvanauskas, G Sucha and R Patel. Novel ultrashort pulse fiber lasers and their applications. Proceedings of SPIE. 2002; 4426:483–488

[4] M I Dzhibladze, Z G Esiashvili, E S Teplitskii, S K Isaev and V R Sagaradze. Mode-locking in a fiber laser. Kvantovaya Elektron. 1983; 10:432–434

[5] V J Matsas and T P Newson. Self starting passively mode locked fibre ring soliton laser exploiting nonlinear polarization rotation. Electron Lett. 1992; 28(15):1391–1393

[6] Doran N J and Wood D, Nonlinear-optical loop mirror. Opt. Lett. 1988; 13(1):56–58

[7] M. E. Fermann, F. Haberl, M. Hofer, and H. Hochreiter, Nonlinear amplifying loop mirror. Opt. Lett. 1990; 15(13):752–754

[8] X Jin, X Wang, X Wang, and P Zhou, Tunable multiwavelength mode-locked Tm/Ho-doped fiber laser based on a nonlinear amplified loop mirror. Appl. Opt. 2015; 54(28): 8260–64

[9] U Keller, K J Weingarten, F X Kartner, et al. Semiconductor saturable absorber mirrors (SESAM's) for femtosecond to nanosecond pulse generation in solid-state lasers. IEEE J. Sel. Top. Quantum Electron. 1996; 2(3):435–453

[10] S Y Set, H Yaguchi, Y Tanaka, and M Jablonski, Ultrafast fiber pulsed lasers incorporating carbon nanotubes. IEEE J. Sel. Top. Quantum Electron. 2004; 10(1):137–146

[11] J Du, Q Wang, G Jiang, et al. Ytterbium-doped fiber laser passively mode locked by few-layer molybdenum disulfide (MoS_2) saturable absorber functioned with evanescent field interaction. Sci. Rep. 2014; 4(4):6346

[12] D Mao, Y Wang, C Ma, L Han, B Jiang, X Gan, S Hua, W Zhang, T Mei, and J Zhao, WS_2 mode-locked ultrafast fiber laser. Sci. Rep. 2015; 5:7965

[13] Y Chen, G Jiang, S Chen, et al. Mechanically exfoliated black phosphorus as a new saturable absorber for both Q-switching and Mode-locking laser operation. Opt. Express. 2015; 23(10):12823–12833

[14] Z Luo,Y Huang, J Weng, et al. 1.06 μm Q-switched ytterbium-doped fiber laser using few-layer topological insulator Bi_2Se_3 as a saturable absorber. Opt. Express. 2013; 21(24) :29516–29522

[15] J Sotor, G Sobon, K Grodecki, et al. Mode-locked erbium-doped fiber laser based on evanescent field interaction with Sb_2Te_3 topological insulator. Appl. Phys. Lett. 2014; 104(25):251112

[16] K Kashiwagi and S Yamashita. Deposition of carbon nanotubes around microfiber via evanescent light. Opt. Express. 2009; 17(20):18364–18370

[17] Z Cheng, H Li, and P Wang. Simulation of generation of dissipative soliton, dissipative soliton resonance and noise-like pulse in Yb-doped mode-locked fiber lasers. Opt. Express. 2015; 23(5):5972–5981

[18] A Ivanenko, S Turitsyn, S Kobsev, and M Dubov. Mode-locking in 25-km fibre laser. in Optical Communication (ECOC), 2010 36th European Conf. and Exhibition on. 2010:1–3

[19] A Hideur, T Chartier, M Brunel, S Louis, C Özkul, and F Sanchez. Generation of high energy femtosecond pulses from a side-pumped Yb-doped double-clad fiber laser. Appl. Phys. Lett. 2001; 79:3389

[20] K Kieu, W H Renninger, A Chong, and F. W. Wise. Sub-100 fs pulses at watt-level powers from a dissipative-soliton fiber laser. Opt. Lett. 2009; 34(5):593–595

[21] Y Huang, Z Luo, F Xiong, Y Li, M Zhong, Z Cai, H Xu, and H Fu. Direct generation of 2 W average-power and 232 nJ picosecond pulses from an ultra-simple Yb-doped double-clad fiber laser. Opt. Lett. 2015; 40(6):1097–1100

[22] H A Haus. Mode-locking of lasers,. IEEE J. Sel. Top. Quant Electron. 2000; 6(6):1173–1185

[23] G P Agrawal. Nonlinear Fiber Optics. 4th ed. San diego, CA. Academic Press; 2009

[24] Z Zhang and G Dai. All-normal-dispersion dissipative soliton ytterbium fiber laser without dispersion compensation and additional filter. IEEE Photon. J. 2011; 3(6):1023–1029

[25] B Sonia, F Christophe, K Huseyin, and P Periklis. Pulse shaping in mode-locked fiber lasers by in-cavity spectral filter. Opt. Lett. 2014; 39(3):438–441

[26] S Yamashita. A tutorial on nonlinear photonic applications of carbon nanotube and graphene. J. Lightwave Technol. 2012; 30(4):427–447.

[27] Y Li and S L Qu. Femtosecond laser-induced breakdown in distilled water for fabricating the helical microchannels array. Opt. Lett. 2011; 36(21):4236–4238

[28] Z Sun, T Hasan, F Wang, A G. Rozhin, I H. White, and A C. Ferrari. Ultrafast stretched-pulse fiber laser mode-locked by carbon nanotubes. Nano Res. 2010; 3:404–411

[29] E J R Kelleher, J C Travers, Z Sun, A G Rozhin, A C Ferrari, S V Popov, and J R Taylor. Nanosecond-pulse fiber lasers mode-locked with nanotubes. Appl. Phys. Lett. 2009; 95(11):111108

[30] S Kobtsev, S Kukarin, and Y Fedotov. Ultra-low repetition rate mode-locked fiber laser with high-energy pulses. Opt. Express. 2008; 16(26):21936–21941

[31] T North and M Rochette. Raman-induced noiselike pulses in a highly nonlinear and dispersive all-fiber ring laser. Opt. Lett. 2013; 38(6):890–892

[32] D Strickland and G Mourou. Compression of amplified chirped optical pulses. Opt. Commun. 1985; 56(6):447–449

[33] M E Fermann and I Hartl. Ultrafast fibre lasers. Nature Photon. 2013; 7:868–874

[34] Y Zaouter, F Guichard, C Hoenninger, et al. High average power 600 uJ ultrafast fiber laser for micromachining application. Journal of Laser Applications. 2015; 27: S29301

[35] G A Ball, C E Holton, G Hull-Allen, and W W Morey. 60 mW 1.5 μm single-frequency low-noise fiber laser MOPA. IEEE J. Photon. Technol. Lett. 1994; 6(2):192–194.

[36] A Malinowski, A Piper, J H V Price, K Furusawa, Y Jeong, J Nilsson, and D J Richardson. Ultrashort-pulse Yb^{3+}-fiber-based laser and amplifier system producing>25-W average power. Opt. Lett. 2004; 29(17):2073–2075

[37] L Zhang, Y G Wang, H J Yu, et al. 20 W high-power picosecond single-walled carbon nanotube based MOPA laser system. J. Lightwave Technol. 2012; 30(16):2713–17

[38] J J Chi, P X Li, H Hu, et al. 120W subnanosecond ytterbium-doped double clad fiber amplifier and its application in supercontinuum generation. Laser Phys. 2014; 24(8): 085103

[39] http://www.ipgphotonics.com/apps_mat_lab_cutting.htm

[40] J Gabzdyl. Application versatility of nanosecond pulsed fiber lasers. Ind Laser Solut. 2014; 29 (1):p4

[41] J Yun, C Gao, S Zhu, C Sun, H He, L Feng, L Dong, et al. High-peak-power, single-mode, nanosecond pulsed, all-fiber laser for high resolution 3D imaging LIDAR system. Chin. Opt. Lett. 2012; 10(12):121402

[42] A Liu, M A Norsen and R D Mead. 60W green output by frequency doubling of polarized Yb-doped fiber laser. Opt. Lett. 2005; 30(1):67–69

[43] N Nishizawa, H Kawagoe and M Yamanaka. Highly functional ultrashort pulse fiber laser sources and applications for optical coherence tomography. CPMT Symposium Japan (ICSJ) 2015, IEEE. Kyoto. 2015: 85–87.

[44] M E Fermann, A Galvanauskas, and G Sucha. Ultrafast lasers: technology and applications. 1st edn. Marcel Dekker AG: CRC Press; 2002

[45] K Sugioka and Y Cheng. Ultrafast lasers—reliable tools for advanced materials processing. Light: Science & Applications. 2014; 3: e149

[46] L Rihakova1 and H Chmelickova. Laser micromachining of glass, silicon, and ceramics. Adv Mater Sci Eng 2015; 2015:584952

[47] I Miyamoto, K Cvecek, Y Okamoto, et al. Internal modification of glass by ultrashort laser pulse and its application to microwelding, Appl. Phys. A. 2014; 114:187–208

[48] N A Inogamov, V V Zhakhovsky, S I Ashitkov, et al. Pump-probe method for measurement of thickness of molten layer produced by ultrashort laser pulse. AIP Conf. Proc. 1278. 2010; 590–599

[49] J M Vadillo and J J Laserna. Laser-induced plasma spectrometry: truly a surface analytical tool. Spectrochim. Acta Part B Atomic Spectroscopy. 2004; 59(2):147–161

[50] D Wu, S Z Wu, J Xu, et al. Hybrid femtosecond laser micro-fabrication to achieve true 3D glass/polymer composite biochips with multiscale features and high performance: the concept of ship-in-a-bottle biochip. Laser Photon. Rev. 2014; 8(3):458–467